Experimental Analysis of Transmission Line Parameters in High-Speed GaAs Digital Circuit Interconnects

Kürşad Kızıloğlu, *Student Member, IEEE*, Nadir Dagli, *Member, IEEE*, George L. Matthaei, *Life Fellow, IEEE*, and Stephen I. Long, *Senior Member, IEEE*

Abstract—**Transmission line properties of typical high-speed interconnects are experimentally investigated by fabricating and characterizing coplanar strips on semi-insulating GaAs substrates. The strips have thicknesses of about 2500 Å or 5000 Å and widths of 4, 6, or 8 μm so as to be representative of on-chip interconnects in high-speed GaAs digital circuits. Measurements are carried out up to 18 GHz, and the pertinent line parameters, such as resistance, capacitance per unit length, and characteristic impedance, are extracted using the measured *S* parameters. The measurement results confirm the quasi-TEM properties of such interconnects. In all cases, the measured distributed capacitance and inductance are insensitive to frequency whereas the resistance is found to increase as much as 38% for the widest and thickest conductors.**

I. Introduction

THE intense research efforts expended on the development of high-speed GaAs digital integrated circuits over the last decade have resulted in high-performance circuits with integration levels exceeding several thousand gates [1]. The continuing improvements in speed and complexity of such circuits, however, generate new problems that must be overcome for further development.

One of these problems is caused by the conductors that interconnect various gates. In high-speed GaAs digital circuits, as a result of the very short rise and fall times of the digital waveforms, frequency components extending well into the microwave range are typically encountered. Furthermore, the average interconnection line length increases with the increasing complexity of the circuitry. Hence some of the interconnect lengths may be comparable to the wavelengths associated with the high-frequency components of the digital waveforms, and undesired wave effects associated with transmission lines, such as distortion and cross talk, can be observed on such interconnects. Therefore, such phenomena could be among the bottlenecks in improving the speed of GaAs digital circuits.

Manuscript received September 5, 1990; revised April 24, 1991. This work was supported by DARPA through the Office of Naval Research under Contract N0014-88-0497.

The authors are with the Department of Electrical and Computer Engineering, University of California, Santa Barbara, CA 93106.

IEEE Log Number 9101369.

In recent years, there has been much theoretical work undertaken to predict the parameters and performance of interconnects in integrated circuits [2]–[9]. On the experimental side, Getsinger proposes different methods for measuring the characteristic impedance of a microstrip line [10]. Shepherd and Daly model and measure the *S* parameters of step-impedance microstrip lines on Duroid board [11]. Gopinath compares a Green's function approach that is used to predict the conductor, dielectric, and radiation losses with measurements of resonator structures on microstrip lines [12]. Lee and Itoh characterize a slow-wave coplanar waveguide structure and compare their measurements with the so-called PEM method [13]. The only available extensive measurements so far that cover a wide range of frequencies for rectangular conductors of different widths and thicknesses are those published by Haefner in 1937 [14]. To our knowledge, however, experimental characterization of such transmission lines as on-chip high-speed GaAs interconnects has not been reported in the literature.

The objective of this research is to provide experimental evidence which will be helpful in validating various possible theoretical approaches to the modeling of such interconnects. Although our emphasis will be on digital circuits, the results can be used for analog applications as well. Our findings show that quasi-TEM theory yields very good qualitative and quantitative results in the frequency range of this investigation.

In the next section the fabrication of representative on-chip GaAs high-speed digital circuit interconnects is described. Next the experimental setup and the method used to extract line parameters from measurement results are outlined. In Section V, the results are discussed; finally, conclusions of this work are given.

II. Fabrication

Various test patterns were designed for an experimental study of the typical interconnects that are encountered in high-speed digital integrated circuits. Most interconnect lines used in practice are coplanar strips on semi-insulating GaAs substrate without a ground plane or at least with the ground plane so far removed compared

0018-9480/91/0800-1361$01.00

with the strip spacings that it has negligible effect on the signal propagation. The aim of the experiments is to measure the essential parameters of these interconnect transmission lines, such as loss, attenuation and propagation constants, characteristic impedance, and phase velocity, as a function of frequency and line dimensions, and to compare these results with approximate theoretical predictions. Fig. 1 shows a schematic of the basic coplanar strip geometry used in the experiments.

Conductor widths (w) of 4, 6, or 8 μm and spacings between the conductors (s) of 4 or 8 μm were used in the experiments. All possible permutations of these w and s values were combined, resulting in line structures of different dimensions. Four different length values (l) of 1, 2, 3, and 4 cm were fabricated for each line. For classification purposes, the notation #_*wsl* was used, where # is the specimen number. At least seven of each of these patterns were fabricated, allowing for possible low yields. The layout of the mask was done using Magic, an integrated circuit layout tool developed at the University of California at Berkeley.

The patterns on the mask were transferred to a 2 in. semi-insulating GaAs wafer about 670 μm thick, using a lift-off technique. Lines with the two thickness values of 2500 Å and 5000 Å were fabricated. The metallization consisted of Au and Ti, the latter to promote the adhesion of Au to GaAs substrate. The Ti thickness was 500 Å for both cases. Conductor thickness measurements on the fabricated samples showed that the thickness of the lines varied between 5300 and 5500 Å for the 5000 Å target and between 2700 and 3000 Å for the 2500 Å one. There was a small offset in the lateral dimensions from the design values caused by a slight offset in the dimensions on the mask itself and also by line width variations in photolithography. Generally, the widths of the lines were larger by abut 0.5 μm, and the spacings were smaller than the design values by the same amount. In the calculations and processing of the measured data, these measured line dimensions were used in place of the nominal design values.

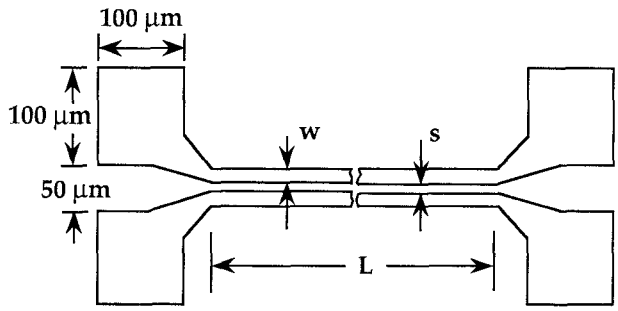

Fig. 1. Schematic of the basic coplanar stripline geometry used in the experiments.

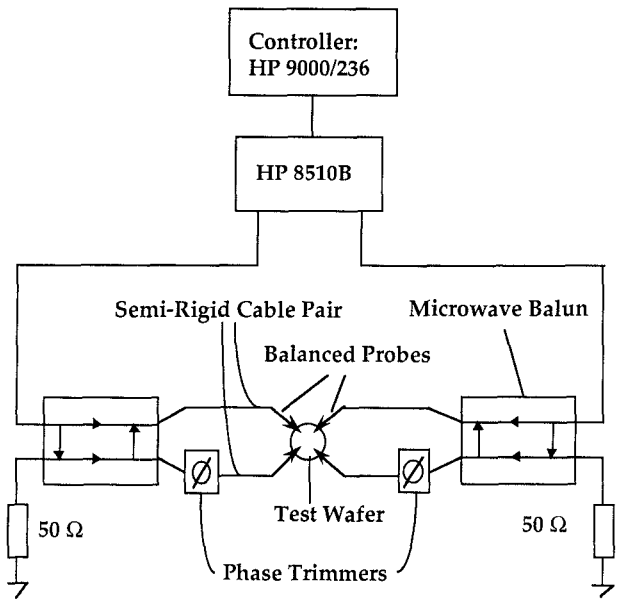

Fig. 2. Schematic of the experimental setup used in the measurements.

III. Measurement Setup

A schematic of the experimental setup used in the measurements is shown in Fig. 2. The microwave measurements on the lines were performed in the 45 MHz–18 GHz frequency range using an HP8510B automatic network analyzer. Transmission lines were probed on wafer using a Cascade Microtech probe station. The lines were excited in a balanced mode (i.e., odd mode) using 3 dB, 180° power dividers (microwave baluns). Two different sets of baluns were used for the measurement frequency range. One covered the 45 MHz–2 GHz range, the other the 2–18 GHz range. This excitation is typical of lines driven by a device connected between them on the surface of the substrate, and the single-mode excitation simplifies the interpretation of the measured data. The balanced signals were transmitted to a pair of high-quality balanced Cascade microwave probes via a pair of phase-matched semirigid coaxial transmission lines. Phase trimmers were also installed at the ends of the semirigid cables to correct for possible nonideal phase match in a pair. To give an idea of how good the match in lengths should be, it suffices to note that a difference in length of 0.5 mm between the cables gives rise to about a 15° phase difference at 20 GHz. Calibration was done and verified using an impedance standard substrate (ISS) supplied by Cascade. Excellent calibration was obtained, with s_{11} and s_{22} less than 0.1 dB for open and short, flat to less than 0.1 dB of its value for the load used, and s_{21} and s_{12} within 0.1 dB of zero dB for through transmission across the whole frequency range.

IV. Analysis of the Measurements

An easy way to analyze the measurement results is to utilize *ABCD* parameter formulation. If we refer to the source and load reference impedances as Z_0 and to the line impedance as Z_{0l}, the *ABCD* matrix of the transmis-

sion line section will be

$$\begin{bmatrix} A & B \\ C & D \end{bmatrix} = \begin{bmatrix} \cosh(\gamma l) & Z_{0l}\sinh(\gamma l) \\ \dfrac{\sinh(\gamma l)}{Z_{0l}} & \cosh(\gamma l) \end{bmatrix} \tag{1}$$

while the *ABCD* parameters are related to the *S* parameters by [15]

$$\begin{bmatrix} A & B \\ C & D \end{bmatrix} = \begin{bmatrix} \dfrac{(1+s_{11})(1-s_{22})+s_{12}s_{21}}{2s_{21}} & Z_0\dfrac{(1+s_{11})(1+s_{22})-s_{12}s_{21}}{2s_{21}} \\ \dfrac{1}{Z_0}\dfrac{(1-s_{11})(1-s_{22})-s_{12}s_{21}}{2s_{21}} & \dfrac{(1-s_{11})(1+s_{22})+s_{12}s_{21}}{2s_{21}} \end{bmatrix}. \tag{2}$$

One finds the characteristic impedance and the propagation constant of the transmission lines as

$$Z_{0l} = \sqrt{\frac{B}{C}} \tag{3a}$$

$$\gamma = \frac{1}{l}\cosh^{-1}(A) = \frac{1}{l}\ln\left(A \pm \sqrt{A^2-1}\right) \tag{3b}$$

where l is the length of the transmission line. In finding γ, the matrix element D can also be used. This was checked in the measurements, and it was found that the γ calculated using the matrix element D yielded the same γ as that found from the matrix element A within the accuracy of the measurements.

The propagation constant γ can further be decomposed to its components as $\gamma = \alpha + j\beta$, where α is the attenuation constant (Np/m) and β is the phase constant (rad/m). Note that in (3b), γ is double valued. The physically meaningful γ value is the one with positive attenuation constant, α. This criterion was used to choose the proper root of (3b).

Based on the previous theoretical estimations [16], we postulate that we can use the well-known quasi-TEM model to describe these interconnects. In the quasi-TEM model, the propagation constant and the characteristic impedance are given by

$$\gamma = \sqrt{(R+j\omega L)(G+j\omega C)} \tag{4a}$$

$$Z_{0l} = \sqrt{\frac{R+j\omega L}{G+j\omega C}} \tag{4b}$$

where R is the resistance per unit length, C is the capacitance per unit length, L is the inductance per unit length, and G is the shunt conductance per unit length, which accounts for the dielectric loss in the transmission line.

Hence, once the two-port S parameters of the line are measured, *ABCD* parameters and γ and Z_{0l} are determined using (2) and (3). Then using γ and Z_{0l}, the transmission line parameters can be extracted with the following formulas. The subscript m is used in the designation of these parameters to denote that they are derived from the measurements:

$$R_m = \mathrm{Re}(\gamma Z_{0l}) \tag{5a}$$

$$L_m = \mathrm{Im}(\gamma Z_{0l})/\omega \tag{5b}$$

$$G_m = \mathrm{Re}(\gamma / Z_{0l}) \tag{5c}$$

$$C_m = \mathrm{Im}(\gamma / Z_{0l})/\omega. \tag{5d}$$

In extracting the line parameters for a geometry of particular cross-sectional dimensions, data from at least six lines of the same cross-sectional dimensions were used. In the case of lines with $w = 4$ μm and $s = 8$ μm, data were taken from ten line measurements. Once the propagation constant, the characteristic impedance, and the distributed parameters of all the transmission lines of the same cross-sectional dimensions were found, their statistical means and standard deviations were calculated. The statistical formulas used are [17]

$$\bar{x} = \frac{1}{N}\sum_{j=1}^{N} x_j \tag{6a}$$

$$\sigma(x_1 \cdots x_N) = \sqrt{\frac{1}{N-1}\sum_{j=1}^{N}(x_j - \bar{x})^2} \tag{6b}$$

for the mean and the standard deviation respectively.

V. Discussions on the Results of the Experiments

The distributed line parameters can also be calculated assuming the quasi-TEM model. Then C becomes the static capacitance per unit length, and is calculated using a simple method of moments approach [18]. In this calculation, the dielectric losses were taken to be zero and the relative permittivity, ϵ_r, of the GaAs substrate to be 13. The thickness of the substrate was taken to be semi-infinite, which should be a good approximation since the line spacings are very close relative to the substrate thickness of 670 μm.

The inductance per unit length, L, can also be represented as

$$L = \frac{\mu_0 \epsilon_0}{C_{\text{air}}} + L_{\text{int}} \tag{7}$$

where the first term is the external inductance contribution. In this expression, C_{air} is the static capacitance per unit length of the structure when dielectrics are replaced by air. L_{int} is the internal inductance of the interconnects which results from magnetic energy storage in the conductors, and it was assumed to be equal to $\mu t/3w$, where t is the thickness and w is the width of the conductor [19], [20]. At least for the lower frequencies, the resistance per unit length, R, can be approximated by the dc resistance

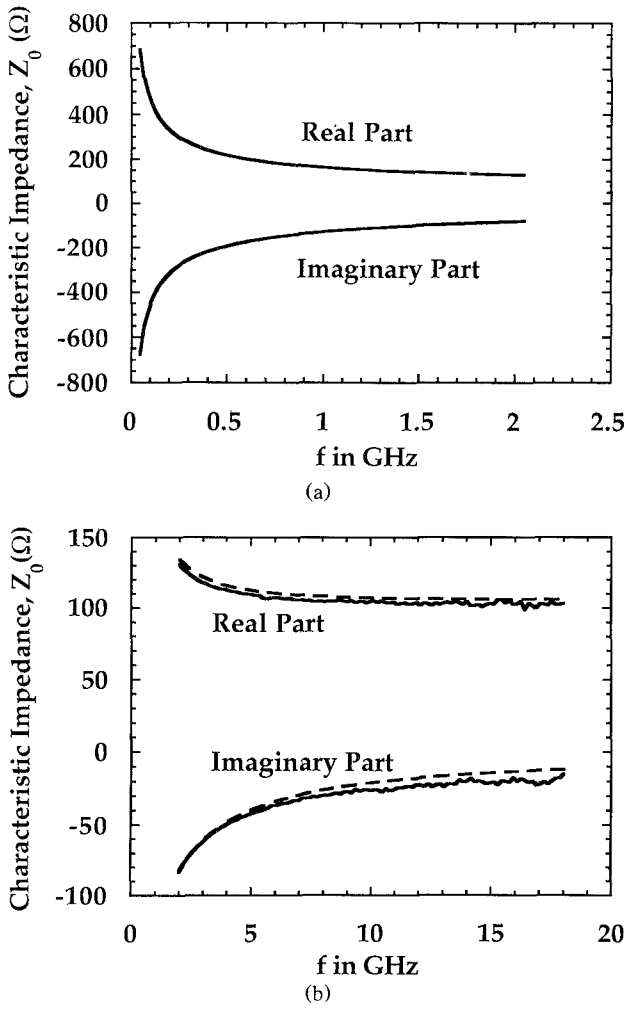

Fig. 3. A comparison between the measured and calculated characteristic impedances for the coplanar strip transmission lines with $w = 4$ μm, $s = 8$ μm, and $t = 0.5$ μm. The dashed lines correspond to the calculated values and the solid lines to the measured values. The calculated values fall exactly on top of the measured ones in (a) and thus are not shown.

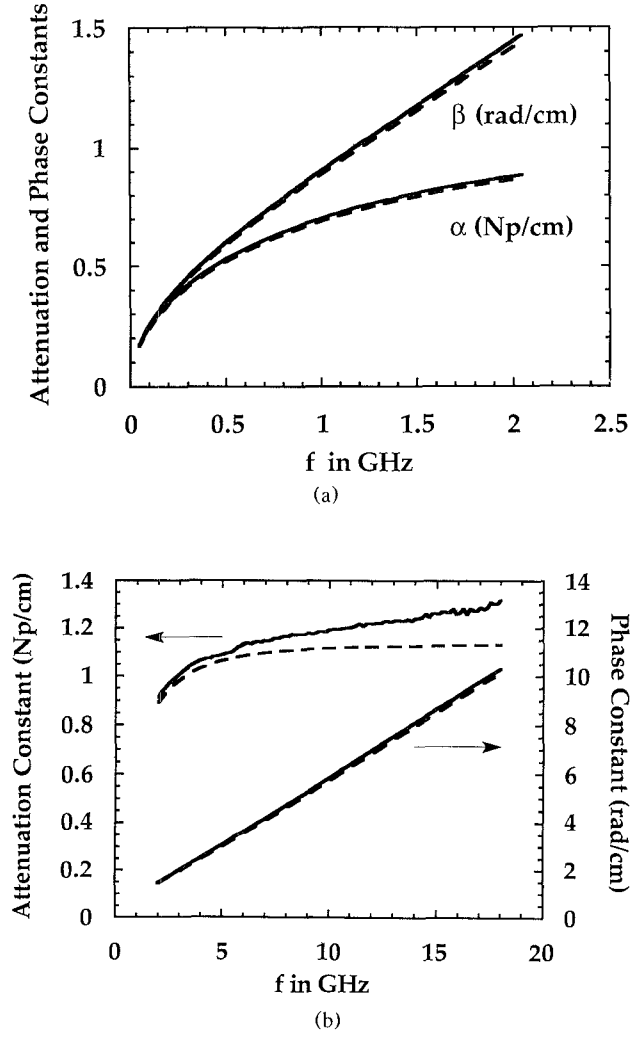

Fig. 4. A comparison of measured and calculated attenuation and propagation constants for lines with $w = 4$ μm, $s = 8$ μm, and $t = 0.5$ μm. The calculated attenuation assumed that the line resistance remains constant at its dc value. Dashed lines are the calculations, and solid lines are the measurements. Note different ordinate scales in (b).

per unit length of these lines; the conductance per unit length, G, is neglected since its effect is believed to be very small compared with ωC in the frequency range of interest.

Figs. 3–8 show the measured parameters for a group of lines together with the values calculated using the method outlined in the previous paragraph. Fig. 3 shows a comparison between the measured and calculated characteristic impedance versus frequency. The behavior of the characteristic impedance can be readily understood by looking at (4b) closely. At low frequencies, ωL can be neglected compared with R, yielding

$$Z_{0l} \approx \frac{1-j}{\sqrt{2}} \sqrt{\frac{R}{\omega C}} . \tag{8}$$

Thus we see that at low frequencies Z_{0l} has equal real and imaginary parts with opposite signs, and these go to infinity as the frequency goes to zero, all of which we observe in Fig. 3(a). At high frequencies, in (4b), R could be neglected compared with ωL since it has a dependence of only $\sqrt{f}$ owing to the skin effect; thus the characteristic impedance should tend toward the real value

$$Z_{0l} \approx \sqrt{\frac{L}{C}} \tag{9}$$

which is observed in Fig. 3(b).

Fig. 4 shows a comparison of the calculated and measured attenuation and phase constants. The attenuation curve varies at low frequencies approximately as $\sqrt{f}$. To understand this behavior, let us consider (4a). Again neglecting the effect of ωL compared with R at low frequencies, the propagation constant becomes

$$\gamma \approx \frac{1+j}{\sqrt{2}} \sqrt{\omega RC} \tag{10}$$

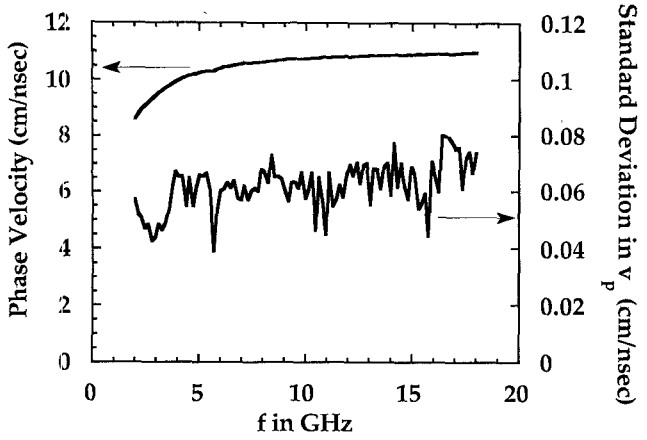

Fig. 5. The measured phase velocity for a group of lines with $w = 4$ μm, $s = 8$ μm, and $t = 0.5$ μm. The calculated high-frequency asymptotic value is $v_p = 1/\sqrt{LC} \approx 11.7$ cm/ns.

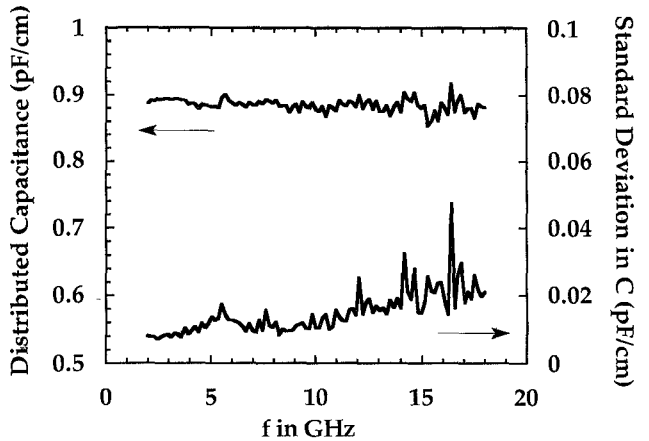

Fig. 6. The capacitance per unit length for the interconnects with $w = 4$ μm, $s = 8$ μm, and $t = 0.5$ μm. The calculated quasi-TEM capacitance value is 0.85 pF/cm.

from which we get the low-frequency α and β as

$$\alpha = \beta = \sqrt{\frac{\omega RC}{2}} . \tag{11}$$

We observe these phenomena in Fig. 4(a).

A second observation on the theoretical attenuation curve in Fig. 4(b) is its relative flatness across the frequency range of interest. To give an explanation for this, we again take (4a) and make a Taylor series expansion of the terms in the square root assuming a situation in which $R/\omega L \ll 1$; in this way we obtain

$$\gamma \approx \frac{R}{2\sqrt{\frac{L}{C}}} + j\omega\sqrt{LC} . \tag{12}$$

The theoretical curve was computed using the constant dc value for R. The higher value for the experimental attenuation is due to an increase in R with frequency, as will be discussed below.

The linearity of β with respect to frequency as observed in Fig. 4(b) is also apparent from (12). We note that the skin depth for gold is approximately $\delta_c \approx 2.5$ μm$/\sqrt{f}$ (GHz). We can assume that the skin effect starts to dominate when $\delta_c \leqslant t/3$, where t is the thickness of the conductor. For our case of $t = 5000$ Å, $\delta_c \approx 1670$ Å would imply $f \approx 225$ GHz, suggesting that we are quite far away from the frequency region where the skin effect starts to dominate.

Another parameter that is directly calculated from the phase constant β is the phase velocity, $v_p = \omega/\beta$. This is shown in Fig. 5. Using (11), it is expected that v_p will go to zero with $\sqrt{f}$ as the frequency tends to zero, a trend which has begun in this figure.

Figs. 6 and 7 show the measured distributed capacitance and inductance per unit length of the transmission lines. The capacitance and inductance look quite frequency independent, with a slight decrease in the inductance as the frequency increases. This may be attributed to the decrease in the internal inductance caused by

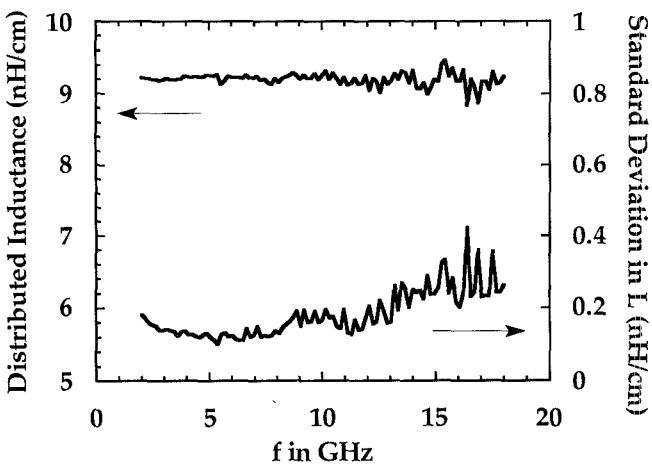

Fig. 7. The measured inductance for the interconnects with $w = 4$ μm, $s = 8$ μm, and $t = 0.5$ μm, which also includes the internal inductance contribution. The calculated quasi-TEM inductance and the low-frequency internal inductance values are 8.50 and 0.93 nH/cm, respectively, giving an expected low-frequency inductance of approximately 9.4 nH/cm.

nonuniform distribution of currents at high frequencies, or, in other words, the decreased penetration of current into the conductor. The close agreement between the calculated and measured capacitance and inductance values justifies the use of quasi-static methods in the calculation of the capacitance, as is done in [18].

Standard deviations of the measured line parameters are also shown in Figs. 5–7. The very small standard deviation values indicate good accuracy and repeatability for the measured values.

Fig. 8 shows the measured resistance variation versus frequency for samples of two different thicknesses, 2500 Å and 5000 Å. For each thickness, two different width values, $w = 4$ μm, and $w = 8$ μm for a separation of $s = 8$ μm were considered. The approximate resistance variations from the low- to the high-frequency end, together with the percentage differences in the high-frequency resistances over the low-frequency values, are given in

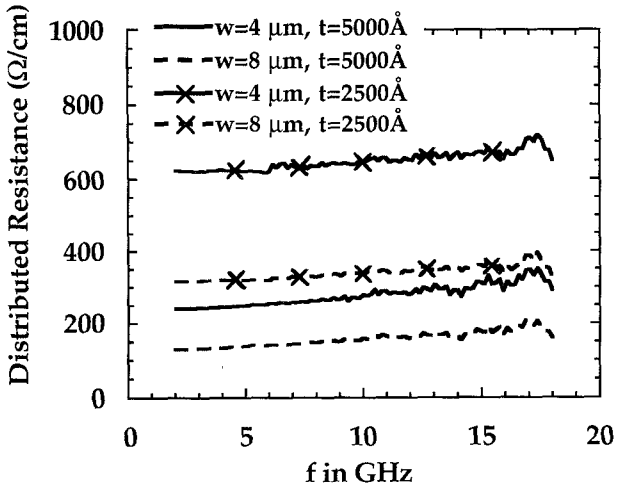

Fig. 8. The distributed resistance for interconnects with $w = 4$ and 8 μm, $s = 8$ μm, and thickness $t = 2500$ Å and 5000 Å.

TABLE I
RESISTANCE VARIATIONS FROM THE LOW TO THE HIGH FREQUENCIES IN THE 2–18 GHz RANGE FOR SAMPLES OF VARIOUS WIDTHS AND THICKNESSES

Sample Width w (μm)	Sample Thickness t (Å)	Range of R (Ω)	Percent Variation in R
4	5000	240–310	29
8	5000	130–180	38
4	2500	620–670	8
8	2500	320–360	12

Table I. The variation of resistance versus frequency increases with wider or thicker strips. The increase in the percent difference is smaller, however, when the strip width is doubled than that when the strip thickness is doubled. From these observations, we can conclude that both the transverse and the vertical distribution of current vary appreciably with frequency within the range of our measurements. The current penetration from the surface decreases as the frequency increases, thereby increasing the line resistance [21], [22]. At very high frequencies, the amount of penetration would be given by the skin depth. Also at high frequencies, current flow should tend to be concentrated near the inner sides of the strips, resulting in higher effective resistance. At least when the thickness is of the order of a skin depth and the strips are several skin depths wide, the frequency dependence of the vertical penetration of current appears to be much larger than that of the lateral distribution of current. One can readily see this by examining Table I. When the width is changed from 4 to 8 μm, the percent variation in the line resistance increases from 8% to 12% for the 2500 Å and from 29% to 38% for the 5000 Å thick lines. However, when the line thickness is increased from 2500 Å to 5000 Å, the percent variation in the line resistance increases from 8% to 29% or from 12% to 38% for the 4 μm and 8 μm widths, respectively.

The extracted shunt conductance per unit length, G, comes out to be quite noisy. This can be attributed to the fact that it has a small value compared with the other parameters and hence is overwhelmed by experimental error. It is therefore not shown.

VI. Conclusions

The analysis of measurements performed on representative interconnect structures reveals several important points. First, the capacitance and inductance come out to be very nearly frequency independent and agree well with the static calculations, which justifies both the use of quasi-static methods in the calculation of capacitance and the assumption of a quasi-TEM model. The slight decrease in the inductance as the frequency increases may be attributed to the decrease of the internal inductance contribution. Furthermore, the propagation and the attenuation constant values calculated using a quasi-TEM model agree both quantitatively and qualitatively with the experimental results.

From the resistance extractions, we observe that both the lateral and the vertical distribution of current must vary significantly with frequency. Within the range of our measurements, the frequency dependence of the narrow vertical distribution, however, is much larger than that of the relatively wide lateral distribution. We also observe that using the dc resistance value of the lines for the calculation of attenuation constant is a very good approximation at low frequencies. For higher frequencies, for example at 10 GHz, this has yielded an error of no more than 8% in the attenuation constant for the experiments carried out so far. This relatively small error in the attenuation assuming frequency-independent resistance should make possible the use of simulation programs such as Spice along with a quasi-TEM transmission line model. For example, in Spice an LC transmission line model could be periodically loaded with a frequency-independent resistance to account for the loss, and hence time-domain analysis of logic gates using reasonably realistic interconnect modeling could be performed.

Acknowledgment

The authors wish to thank Dr. B. Hughes of Hewlett-Packard for fruitful discussions about a direct extraction method.

References

[1] G. Lee, S. Canaga, B. Terrell, and I. Deyhimy, "A high performance GaAs gate array family," *Proc. IEEE GaAs IC Symp.* (San Diego, CA), Oct. 1989, pp. 33–36.
[2] P. Waldow and I. Wolff. "The skin-effect at high frequencies," *IEEE Trans. Microwave Theory Tech.*, vol. MTT-33, pp. 1076–1082, Oct. 1985.
[3] U. Ghoshal and L. N. Smith. "Finite element analysis of skin effect in copper interconnects at 77 K and 300 K," in *1988 IEEE MTT-S Int. Microwave Symp. Dig.*, pp. 773–776.
[4] T. E. van Deventer, P. B. Katehi, and A. C. Cangellaris. "High frequency conductor and dielectric losses in shielded microstrip," in *1989 IEEE MTT-S Int. Microwave Symp. Dig.*, pp. 919–922.
[5] H. Y. Lee and T. Itoh. "Phenomenological loss equivalence method for planar quasi-TEM transmission lines with a thin normal conduc-

tor or superconductor," *IEEE Trans. Microwave Theory Tech.*, vol. 37, pp. 1904–1909, Dec. 1989.
[6] A. R. Djordjevic, T. K. Sarkar, and S. M. Rao, "Analysis of finite conductivity cylindrical conductors excited by axially-independent TM electromagnetic field," *IEEE Trans. Microwave Theory Tech.*, vol. MTT-33, pp. 960–966, Oct. 1985.
[7] J. Venkataraman, S. M. Rao, A. R. Djordjevic, T. K. Sarkar, and Y. Naiheng, "Analysis of arbitrarily oriented microstrip transmission lines in arbitrarily shaped dielectric media over a finite ground plane," *IEEE Trans. Microwave Theory Tech.*, vol. MTT-33, pp. 952–959, Oct. 1985.
[8] F. Medina and M. Horno, "Capacitance and inductance matrices for multistrip structures in multilayered anisotropic dielectrics," *IEEE Trans. Microwave Theory Tech.*, vol. MTT-35, pp. 1002–1008, Nov. 1987.
[9] A. R. Djordjevic, R. F. Harrington, T. K. Sarkar, and M. Bazdar, *Matrix Parameters for Multiconductor Transmission Lines: Software and User's Manual*. Norwood, MA: Artech House, 1989.
[10] W. J. Getsinger, "Measurement and modeling of the apparent characteristic impedance of microstrip," *IEEE Trans. Microwave Theory Tech.*, vol. MTT-31, pp. 624–632, Aug. 1983.
[11] P. R. Shepherd and P. Daly, "Modeling and measurement of microstrip transmission-line structures," *IEEE Trans. Microwave Theory Tech.*, vol. MTT-33, pp. 1501–1506, Dec. 1985.
[12] A. Gopinath, "Losses in coplanar wavequides," *IEEE Trans. Microwave Theory Tech.*, vol. MTT-30, pp. 1101–1104, July 1982.
[13] H. Y. Lee and T. Itoh, "Experimental and theoretical characterization of very thin coplanar waveguide and coplanar slow-wave structures," in *1990 IEEE MTT-S Int. Microwave Symp. Dig.*, pp. 175–178.
[14] S. J. Haefner, "Alternating-current resistance of rectangular conductors," *Proc. IRE*, vol. 25, pp. 435–447, Apr. 1937.
[15] G. Gonzales, *Microwave Transistor Amplifiers*. Englewood Cliffs, NJ: Prentice-Hall, 1984, p. 25.
[16] G. L. Matthaei, K. Kızıloğlu, N. Dagli, and S. I. Long, "The nature of the charges, currents, and fields in and about conductors having cross-sectional dimensions of the order of a skin depth," *IEEE Trans. Microwave Theory Tech.*, vol. 38, pp. 1031–1036, Aug. 1990.
[17] W. H. Press, B. P. Flannery, S. A. Teukolsky, and W. T. Vetterling, *Numerical Recipes: The Art of Scientific Computing*. Cambridge, U.K.: Cambridge University Press, 1986, pp. 455–456.
[18] G. L. Matthaei, G. Chinn, C. Plott, and N. Dagli, "A simplified means for computation of interconnect distributed capacitances and inductances," *IEEE Trans. Computer-Aided Design*, to be published..
[19] R. L. Kautz, "Miniaturization of normal-state and superconducting striplines," *J. Res. Nat. Bur. Stand.*, vol. 84, no. 3, pp. 247–259, May–June 1979.
[20] K. Kızıloğlu, "Modelling and measurement of wave effects in high-speed GaAs digital circuit interconnects," Master's thesis, University of California, Santa Barbara, 1990, section 2.4.
[21] R. Faraji-Dana, and Y. L. Chow, "AC resistance of two coupled strip conductors," *Proc. Inst. Elec. Eng.*, pt. H (*Microwaves, Antennas and Prop.*), vol. 138, no. 1, pp. 37–45, Feb. 1991.
[22] R. Faraji-Dana and Y. L. Chow, "The current distribution and ac resistance of a microstrip structure," *IEEE Trans. Microwave Theory Tech.*, vol. 38, pp. 1268–1277, Sept. 1990.

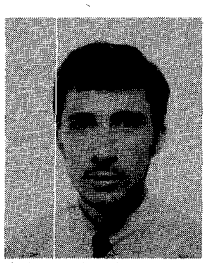

Kürşad Kızıloğlu (S'89) was born in Ankara, Turkey, in 1966. He received the B.S. degree in electrical and electronics engineering (with high honors) from the Middle East Technical University, Ankara, in 1988 and the M.S. degree in electrical engineering in 1990 from the University of California, Santa Barbara, where he is now pursuing the Ph.D. degree. He is currently working on ways of incorporating focused ion beam implantation techniques to obtain specific electronic characteristics of advanced submicron devices.

Mr. Kızıloğlu was awarded an MTT-S Graduate Student Fellowship in 1990.

Nadir Dagli (S'77–M'86) was born in Ankara, Turkey. He received the B.S. and M.S. degrees in electrical engineering from the Middle East Technical University, Ankara, Turkey, in 1976 and 1979, respectively, and the Ph.D. degree, also in electrical engineering, from the Massachusetts Institute of Technology, Cambridge, in 1986. During his Ph.D. research he worked on the design, fabrication, and modeling of guided-wave integrated optical components in III–V compound semiconductors. He also worked on III–V materials preparation by LPE and the modeling and analysis of heterojunction bipolar transistors for microwave and millimeter-wave applications.

He is currently an Assistant Professor at the University of California, Santa Barbara. His current interests are the design, fabrication, and modeling of guided-wave components for optical integrated circuits, solid-state microwave and millimeter-wave devices, electron waveguides, and novel quantum interference devices based on electron waveguides.

Dr. Dagli was awarded NATO science and IBM predoctoral fellowships during his graduate studies. He was the recipient of a 1990 UCSB Alumni Distinguished Teaching Award and of a 1990 UC Regents Junior Faculty Fellowship.

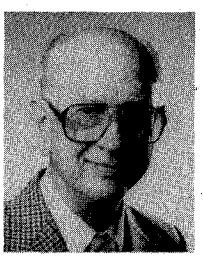

George L. Matthaei (S'49–A'52–M'57–F'65–LF'89) received the B.S. degree from the University of Washington in 1948 and the Ph.D degree from Stanford University in 1952.

From 1951 to 1955, he was on the faculty of the University of California, Berkeley, where he was an Assistant Professor, and his specialty was network synthesis. From 1955 to 1958, he was engaged in system analysis and microwave component research at the Ramo-Wooldridge Corporation. From 1958 to 1964, he was at Stanford Research Institute, where he was engaged in microwave device research and became Manager of the Electromagnetic Techniques Laboratory in 1962. In July 1964, he joined the Department of Electrical Engineering at the University of California, Santa Barbara, where he is a Professor. He is the author of numerous papers, coauthor of the book *Microwave Filters, Impedance-Matching Networks and Coupling Structures*, and a contributor to several other books. His current interests are in the areas of cross talk and wave effects in digital circuits, and microwave and millimeter-wave passive and active circuits.

Dr. Mathaei is a member of Tau Beta Pi, Sigma Xi, and Eta Kappa Nu. He was a winner of the 1961 Microwave Prize of the IEEE MTT Group. In 1984 he received an IEEE Centennial Medal and in 1986 was the recipient of the Microwave Career Award of the IEEE Microwave Theory and Techniques Society.

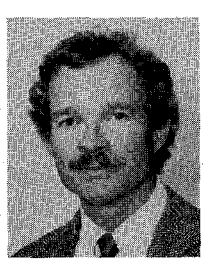

Stephen I. Long (S'68–M'73–SM'80) received the B.S. degree in engineering physics from the University of California, Berkeley, in 1967, and the M.S. and Ph.D. degrees in electrical engineering from Cornell University, Ithaca, NY, in 1969 and 1974, respectively. His thesis research dealt with steady-state liquid phase epitaxial growth of GaAs.

From 1974 to 1977 he was a Senior Engineer and Manager of Semiconductor Engineering at Varian Associates, Palo Alto, CA, where he was involved in the development of vapor phase epitaxial growth of GaAs and InP, design and development of high-efficiency GaAs IMPATT devices, millimeter-wave InP Gunn devices, and project management. From 1978 to 1981 he was employed by Rockwell International, Thousand Oaks, CA, where he contributed to the design, modeling, and characterization of high-speed GaAs MSI/LSI digital integrated circuits and to project management. In 1981 he joined the Electrical and Computer Engineering Department of the University of California, Santa Barbara, where he is currently a Professor. His research interests are in the design and fabrication of high-speed III–V semiconductor devices and GaAs digital and analog integrated circuits.

Dr. Long is a member of Tau Beta Pi. In 1978 he received the IEEE Microwave Applications Award for his development of InP millimeter-wave devices. In 1988 he was a research visitor at the GEC Hirst Research Centre, U.K.